Magnetic Odometry - A Model-Based Approach Using A Sensor Array

Isaac Skog, Gustaf Hendeby and Fredrik Gustafsson

N.B.: When citing this work, cite the original publication.
Skog, I., Hendeby, G., Gustafsson, F., (2018), Magnetic Odometry - A Model-Based Approach Using A Sensor Array, *2018 21st International Conference on Information Fusion (FUSION)*, , 794-798.
https://doi.org/10.23919/ICIF.2018.8455430

Original publication available at:
https://doi.org/10.23919/ICIF.2018.8455430

Magnetic Odometry – A Model-Based Approach Using A Sensor Array

Isaac Skog, Gustaf Hendeby, and Fredrik Gustafsson
Dept. of Electrical Engineering, Linköping University, Linköping, Sweden
e-mail: firstname.lastname@liu.se

***Abstract*—A model-based method to perform odometry using an array of magnetometers that sense variations in a local magnetic field is presented. The method requires no prior knowledge of the magnetic field, nor does it compile any map of it. Assuming that the local variations in the magnetic field can be described by a curl and divergence free polynomial model, a maximum likelihood estimator is derived. To gain insight into the array design criteria and the achievable estimation performance, the identifiability conditions of the estimation problem are analyzed and the Cramér-Rao bound for the one-dimensional case is derived. The analysis shows that with a second-order model it is sufficient to have six magnetometer triads in a plane to obtain local identifiability. Further, the Cramér-Rao bound shows that the estimation error is inversely proportional to the ratio between the rate of change of the magnetic field and the noise variance, as well as the length scale of the array. The performance of the proposed estimator is evaluated using real-world data. The results show that, when there are sufficient variations in the magnetic field, the estimation error is of the order of a few percent of the displacement. The method also outperforms current state-of-the-art method for magnetic odometry.**

I. Introduction

A model-based method to perform odometry using an array of magnetometers that sense variations in a local magnetic field is presented. In contrast to magnetic field based simultaneous localization and mapping (SLAM) and fingerprinting solutions, as represented by [1] and [2], the proposed method requires no prior knowledge of the magnetic field, nor does it compile any magnetic field map over time. Hence, the proposed method can e.g., be used to increase the positioning accuracy during the exploration phase of a magnetic SLAM process or in applications where the computational and memory resources prevent the construction and storage of a magnetic field map.

The idea that the velocity of an object can be estimated by equipping it with a magnetometer array that observes the variations in the local magnetic field was introduced in [3]. The idea is based upon the differential equation

$$\frac{d\mathbf{m}}{dt} = \mathbf{m} \times \boldsymbol{\omega} + \frac{d\mathbf{m}}{d\mathbf{r}}\mathbf{v}, \tag{1}$$

which relates the rate of change of the magnetic field $\mathbf{m} \in \mathbb{R}^3$ to the rotation rate of the array $\boldsymbol{\omega} \in \mathbb{R}^3$ (assumed to be measured by a gyroscope triad in [3]), the Jacobian of the magnetic field $d\mathbf{m}/d\mathbf{r} \in \mathbb{R}^{3,3}$, and the velocity $\mathbf{v} \in \mathbb{R}^3$; all quantities are expressed with respect to the array coordinate frame. With an assembly of spatially distributed magnetometers, also known as a magnetometer array, the Jacobian $d\mathbf{m}/d\mathbf{r}$ can be estimated and the differential equation solved. That is, the velocity $\mathbf{v}$ can be estimated. Note that this is the velocity in the array frame and without further information regarding the orientation of the array it can only be used to determine the speed of the array in a fixed frame of reference. An example of a sensor array that can be used to perform magnetic odometry is shown in Fig. 1.

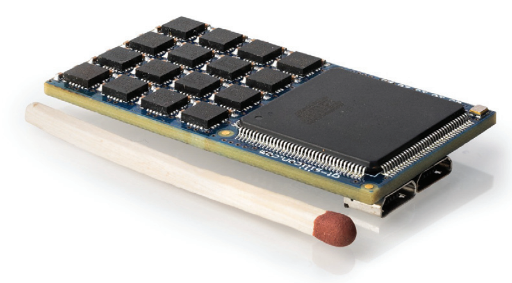

Fig. 1. Sensor array made out of 32 MPU 9150 InvenSense sensor modules, each holding a magnetometer triad. Details regarding the array can be found at http://www.openshoe.org.

In paper [3] and in the subsequent work [4] and [5] by the same authors, as well as in the recent paper [6], the differential equation (1) is used to develop a speed aided inertial navigation system. The result is a positioning system with much slower error growth rate than a pure inertial navigation system; theoretically, the errors should grow linearly with time, instead of cubically. Indeed, the experimental results presented in [5] show that in an environment where there are sufficient variations in the magnetic field, such a magnetic odometry aided inertial navigation system can achieve a position error proportional to a few percent of the distance traveled.

In this paper, the velocity of the array is not estimated by directly solving (1). Instead the velocity estimation is viewed as a model parameter estimation problem where a signal model that has the velocity as a free parameter is fitted to the observed data. This allows the application of estimation theoretical tools to analyze the properties of the magnetic odometry problem and to derive various estimators for the displacement. Further, the proposed method makes it straightforward to use higher order models to describe the magnetic field variations, which enable a more accurate displacement estimation. Moreover, in the proposed method both the translational and rotational

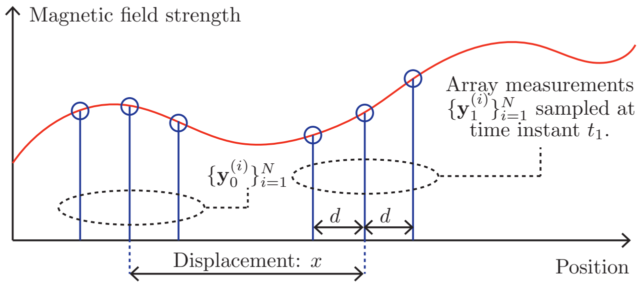

Fig. 2. Illustration (in one dimension) of the idea behind the model-based approach to displacement (speed) estimation using variations in the magnetic field. Given the measurements $\{\mathbf{y}_0^{(i)}\}_{i=1}^N$ and $\{\mathbf{y}_1^{(i)}\}_{i=1}^N$ from the magnetometer sensor array, a local model for the magnetic field is constructed and the displacement $\mathbf{x}$ that best fits this model is estimated.

motion of the array can be estimated without any gyroscopes, which makes it possible to perform dead-reckoning using only an array of magnetometers.

The outline of the paper is as follows. First, a signal model for the magnetic field measurements is presented in Section II. Secondly, in Section III, a maximum likelihood estimator for the displacement of the array is presented. The identifiability conditions and Cramér-Rao for the estimation problem are also analyzed. Thirdly, in Section IV, the performance of the estimator is experimentally evaluated and compared to the case when the displacement is estimated by directly solving (1). Finally, in Section V, the results are summarized and conclusions drawn.

II. Signal Model

In this section, a model for the measurements obtained from a magnetometer array moving through a spatially varying magnetic field, as illustrated in Fig. 2, is derived.

A. Prerequisite

With reference to Fig. 2, assume a sensor array consisting of N magnetometer triads that collects the measurement sets $\{\mathbf{y}_0^{(i)}\}_{i=1}^N$ and $\{\mathbf{y}_1^{(i)}\}_{i=1}^N$, at time instant $t_0 \in \mathbb{R}^+$ and $t_1 \in \mathbb{R}^+$, respectively. Here $\mathbf{y}_k^{(i)} \in \mathbb{R}^3$ denotes the measurement at time instant t_k of the i^{th} magnetometer triad. Further, assume that during the time interval $\Delta t \triangleq t_1 - t_0$ the array has undergone the translation $\mathbf{x} = \mathbf{v}\Delta t$ and the rotation described by the Euler angles $\boldsymbol{\phi} \in \mathbb{SO}(3)$.

Next, assume that within the volume $\boldsymbol{\Omega}_{\mathbf{r}}$, centered at the origin of the array at time t_0, the magnetic field can be described by the model $\mathbf{M}(\mathbf{r};\theta)$. Here $\mathbf{r} \in \mathbb{R}^3$ and $\theta \in \mathbb{R}^L$ denote the position within the volume $\boldsymbol{\Omega}_{\mathbf{r}}$ and the model parameters, respectively. Further, assume that the displacement is such that for $i = 1,\dots,N$ it holds that $(\mathbf{x} + \mathbf{R}^\top(\boldsymbol{\phi})\mathbf{d}^{(i)}) \in \boldsymbol{\Omega}_{\mathbf{r}}$. Here $\mathbf{d}^{(i)} \in \mathbb{R}^3$ denotes the position of the i^{th} sensors in the array and $\mathbf{R}(\boldsymbol{\phi}) \in \mathbb{SO}(3)$ denotes the rotation matrix parameterized by the Euler angles $\boldsymbol{\phi}$. The measurements in the two sets $\{\mathbf{y}_0^{(i)}\}_{i=1}^N$ and $\{\mathbf{y}_1^{(i)}\}_{i=1}^N$ can then be modeled as

$$\mathbf{y}_0^{(i)} = \mathbf{M}(\mathbf{d}^{(i)};\boldsymbol{\theta}) + \mathbf{e}_0^{(i)} \tag{2a}$$

$$\mathbf{y}_1^{(i)} = \mathbf{R}(\boldsymbol{\phi})\mathbf{M}(\mathbf{x} + \mathbf{R}^\top(\boldsymbol{\phi})\mathbf{d}^{(i)};\boldsymbol{\theta}) + \mathbf{e}_1^{(i)}. \tag{2b}$$

Here $\mathbf{e}_k^{(i)} \in \mathbb{R}^3$ denotes the measurement error of the i^{th} sensor triad.

If the array moves in a static magnetic field with no free current then, according to Maxwell's equations, the field should be both curl and divergence free [7]. Hence, the magnetic field model $\mathbf{M}(\mathbf{r};\boldsymbol{\theta})$ per design, or via the choice of model parameter values, should satisfy the conditions

$$\nabla_{\mathbf{r}} \times \mathbf{M}(\mathbf{r};\boldsymbol{\theta}) = \mathbf{0} \tag{3a}$$

$$\nabla_{\mathbf{r}} \cdot \mathbf{M}(\mathbf{r};\boldsymbol{\theta}) = \mathbf{0} \tag{3b}$$

for all $\mathbf{r} \in \boldsymbol{\Omega}_{\mathbf{r}}$. Next, a polynomial model will be designed that fulfills these conditions.

B. Polynomial Magnetic Field Model

One way to create an ℓ^{th} order polynomial model of a curl free field is to describe the scalar potential $\varphi(\mathbf{r})$ as an $(\ell+1)^{\text{th}}$ order polynomial and then define the magnetic field as the gradient of the potential. That is, the scalar potential is modelled by the polynomial

$$\varphi(\mathbf{r}) = \mathbf{h}(\mathbf{r})^\top\boldsymbol{\theta} + c, \tag{4}$$

where $\mathbf{h}(\mathbf{r})$ is a vector whose elements are given by the product $r_x^i r_y^j r_z^k$ for $\forall\{i,j,k\} \in \mathbb{N}$, subject to $1 \leq i + j + k \leq m$, $m = 1,\dots,\ell+1$. Further, c is an arbitrary constant and the model parameters $\boldsymbol{\theta}$ make up the polynomial coefficients. The number of model parameters is in this case $L = (\ell+4)(\ell+3)(\ell+2)/6 - 1$. The magnetic field is then given by

$$\mathbf{M}(\mathbf{r};\boldsymbol{\theta}) = \nabla_{\mathbf{r}}\varphi(\mathbf{r}) = \mathbf{A}(\mathbf{r})\boldsymbol{\theta}, \tag{5}$$

where $\mathbf{A}(\mathbf{r}) \triangleq \nabla_{\mathbf{r}}\mathbf{h}(\mathbf{r})^\top$. By design the magnetic field described by the model in (5) is curl free $\forall\boldsymbol{\theta} \in \mathbb{R}^L$; hence requirement (3a) is fulfilled.

To ensure that the magnetic field is divergence free, the parameters $\boldsymbol{\theta}$ must be chosen such that

$$\nabla_{\mathbf{r}} \cdot \mathbf{A}(\mathbf{r})\boldsymbol{\theta} = \sum_{i=x,y,z} \frac{d[\mathbf{A}(\mathbf{r})\boldsymbol{\theta}]_i}{dr_i} = 0 \quad \forall\mathbf{r} \in \boldsymbol{\Omega}_{\mathbf{r}}. \tag{6}$$

Here $d[\mathbf{A}(\mathbf{r})\boldsymbol{\theta}]_i/dr_i$ is an $(\ell-1)^{\text{th}}$ order polynomial in three variables. Therefore, for the equality in (6) to hold $\forall\mathbf{r} \in \boldsymbol{\Omega}_{\mathbf{r}}$ the coefficients for each power in the sum of the three polynomials must sum to zero. Hence, the constraint in (6) can equivalently be written as a system of $K = (\ell+2)(\ell+1)\ell/6$ equations. Let $\mathbf{B}\boldsymbol{\theta} = \mathbf{0}$ denote this system of equations, then a curl and divergence free ℓ^{th} order polynomial model for the magnetic field is given by

$$\mathbf{M}(\mathbf{r};\boldsymbol{\theta}) = \mathbf{A}(\mathbf{r})\boldsymbol{\theta}, \qquad \forall\boldsymbol{\theta} \in \mathbb{R}^L \quad \text{s.t.} \quad \mathbf{B}\boldsymbol{\theta} = \mathbf{0}. \tag{7}$$

This model can be reparameterized as a lower order model by introducing the matrix $\mathbf{B}^\perp \triangleq \text{null}\{\mathbf{B}\}$ whose columns spans the null space of $\mathbf{B}$, and then setting $\boldsymbol{\theta} = \mathbf{B}^{\perp}\boldsymbol{\theta}_l$, where $\boldsymbol{\theta}_l \in \mathbb{R}^{L-K}$. (The null space matrix can be found via a QR-factorization of the matrix $\mathbf{B}$, see e.g., [8].) The curl and divergence free ℓ^{th} order polynomial model for the magnetic field, expressed in terms of the new parameters $\boldsymbol{\theta}_l$, is then defined by

$$\mathbf{M}(\mathbf{r};\boldsymbol{\theta}_l) \triangleq \mathbf{A}(\mathbf{r})\mathbf{B}^{\perp}\boldsymbol{\theta}_l, \qquad \forall \boldsymbol{\theta}_l \in \mathbb{R}^{L-K}. \tag{8}$$

C. Measurement Model

Given the magnetic field model in (8), the measurement sets $\{\mathbf{y}_0^{(i)}\}_{i=1}^N$ and $\{\mathbf{y}_1^{(i)}\}_{i=1}^N$ can be described by the measurement model

$$\mathbf{z} = \mathbf{H}(\boldsymbol{\theta}_n)\boldsymbol{\theta}_l + \boldsymbol{\eta} \tag{9a}$$

where

$$\mathbf{z} \triangleq \begin{bmatrix} \mathbf{y}_0^{(1)} \\ \vdots \\ \mathbf{y}_0^{(N)} \\ \mathbf{y}_1^{(1)} \\ \vdots \\ \mathbf{y}_1^{(N)} \end{bmatrix}, \quad \boldsymbol{\eta} \triangleq \begin{bmatrix} \mathbf{e}_0^{(1)} \\ \vdots \\ \mathbf{e}_0^{(N)} \\ \mathbf{e}_1^{(1)} \\ \vdots \\ \mathbf{e}_1^{(N)} \end{bmatrix}, \tag{9b}$$

and

$$\mathbf{H} \triangleq \begin{bmatrix} \mathbf{H}_l \\ --- \\ \mathbf{H}_n(\boldsymbol{\theta}_n) \end{bmatrix} = \begin{bmatrix} \mathbf{A}(\mathbf{d}^{(1)})\mathbf{B}^{\perp} \\ \vdots \\ \mathbf{A}(\mathbf{d}^{(N)})\mathbf{B}^{\perp} \\ ------------- \\ \mathbf{R}(\boldsymbol{\phi})\mathbf{A}(\mathbf{x} + \mathbf{R}^{\top}(\boldsymbol{\phi})\mathbf{d}^{(1)})\mathbf{B}^{\perp} \\ \vdots \\ \mathbf{R}(\boldsymbol{\phi})\mathbf{A}(\mathbf{x} + \mathbf{R}^{\top}(\boldsymbol{\phi})\mathbf{d}^{(N)})\mathbf{B}^{\perp} \end{bmatrix}. \tag{9c}$$

Here, $\boldsymbol{\theta}_n = \mathbf{x}$ or $\boldsymbol{\theta}_n = \begin{bmatrix}\mathbf{x}^{\top} & \boldsymbol{\phi}^{\top}\end{bmatrix}^{\top}$ depending upon whether the rotation $\boldsymbol{\phi}$ is assumed to be known or not. Assuming that the magnetometers have been calibrated, the measurement error can be assumed to be zero-mean Gaussian distributed with covariance matrix $\text{cov}(\boldsymbol{\eta}) = \sigma^2\mathbf{I}$. Here σ^2 denotes the variance of the measurement noise.

D. Identifiability Analysis

The measurement model in (9a) has $\dim(\boldsymbol{\theta}_l) + \dim(\boldsymbol{\theta}_n) = L - K + \dim(\boldsymbol{\theta}_n) = \ell^2 + 4\ell + 3 + \dim(\boldsymbol{\theta}_n)$ free parameters; recall, ℓ was the order of the polynomial model. Thus, a necessary condition for the parameters to be uniquely identifiable is that the number of magnetometer triads

$$N \geq \lceil (\ell^2 + 4\ell + 3 + \dim(\boldsymbol{\theta}_n))/6 \rceil. \tag{10}$$

Hence, for a second order polynomial model, i.e., $\ell = 2$, the array must consist of at least three magnetometer triads if the rotation is assumed to be known. If the rotation is unknown, at least four magnetometer triads are needed.

A nonlinear model of the kind in (9a) is said to be locally identifiable if the matrix

$$\boldsymbol{\Pi} \triangleq \begin{bmatrix} \frac{d\mathbf{H}(\boldsymbol{\theta}_n)\boldsymbol{\theta}_l}{d\boldsymbol{\theta}_l} & \frac{d\mathbf{H}(\boldsymbol{\theta}_n)\boldsymbol{\theta}_l}{d\boldsymbol{\theta}_n} \end{bmatrix} = \begin{bmatrix} \mathbf{H}_l & \mathbf{0} \\ \mathbf{H}_n(\boldsymbol{\theta}_n) & \frac{d\mathbf{H}(\boldsymbol{\theta}_n)\boldsymbol{\theta}_l}{d\boldsymbol{\theta}_n} \end{bmatrix} \tag{11}$$

has full rank [9]. Due to the triangular structure of the matrix, $\text{rank}(\boldsymbol{\Pi}) \geq \text{rank}(\mathbf{H}_l) + \text{rank}(\frac{d\mathbf{H}(\boldsymbol{\theta}_n)\boldsymbol{\theta}_l}{d\boldsymbol{\theta}_n})$. Next, utilizing this structure, a sufficient condition, with respect to the array geometry, for the problem to be locally identifiable in the case when $\ell = 2$ will be studied.

It is possible to show, via straightforward but lengthy calculations, that with six magnetometer triads placed in the planar grid

$$\begin{aligned} \mathbf{d}^{(1)} &= \begin{bmatrix}0 & 0 & 0\end{bmatrix}^{\top} & \mathbf{d}^{(2)} &= \begin{bmatrix}-\alpha & 0 & 0\end{bmatrix}^{\top} & \mathbf{d}^{(3)} &= \begin{bmatrix}\alpha & 0 & 0\end{bmatrix}^{\top} \\ \mathbf{d}^{(4)} &= \begin{bmatrix}0 & \alpha & 0\end{bmatrix}^{\top} & \mathbf{d}^{(5)} &= \begin{bmatrix}0 & -\alpha & 0\end{bmatrix}^{\top} & \mathbf{d}^{(6)} &= \begin{bmatrix}\alpha & \alpha & 0\end{bmatrix}^{\top} \end{aligned} \tag{12}$$

where $\alpha \neq 0$, the matrix $\mathbf{H}_l$ has full rank. This implies that the coefficients $\boldsymbol{\theta}_l$, which describe the magnetic field, can be identified from the observations $\{\mathbf{y}_0^{(i)}\}_{i=1}^N$ alone. By not restricting the sensors to be in a plane, it is possible to reduce the number of sensor triads needed to five by, e.g., changing the location of the fifth triad to $\mathbf{d}^{(5)} = \begin{bmatrix}0 & \alpha & \alpha\end{bmatrix}^{\top}$ and removing the sixth triad. It is worth noting that in [10] it is shown that for a linear model, i.e., $\ell = 1$, it sufficient to have three non-collinear magnetometer triads to estimate the model parameters $\boldsymbol{\theta}_l$.

Regarding the identifiability of $\boldsymbol{\theta}_n$, it is possible to show that, given the parameters describing the field $\boldsymbol{\theta}_l$, the displacement of a single magnetometer triad is identifiable if the magnetic field is sufficiently exciting, i.e., any small change in location causes a change in the magnetic field. Since the orientation of a rigid object can be determined from the position of three non-collinear points on the object, this also implies that the orientation of the array can be determined from the measurements $\{\mathbf{y}_1^{(i)}\}_{i=1}^N$. Hence, with a second order model, it is sufficient to have an array with six magnetometer triads in a planar geometry to obtain local identifiablity for all parameters in the signal model.

III. Estimator and Performance Bound

For a separable linear model such as the one in (9a) with Gaussian distributed measurement noise, the maximum likelihood estimator and the Cramér-Rao bound for the nonlinear parameters $\boldsymbol{\theta}_n$ are readily available; the linear parameters are nuisance parameters.

A. Maximum Likelihood Estimator

The maximum likelihood estimator is given by [11] as

$$\hat{\boldsymbol{\theta}}_n = \arg\max_{\boldsymbol{\theta}_n} \mathbf{z}^{\top}\mathbf{P}\mathbf{z}, \tag{13}$$

where the projection matrix $\mathbf{P} = \mathbf{H}(\mathbf{H}^{\top}\mathbf{H})^{-1}\mathbf{H}^{\top}$. The maximization in (13) can be solved using standard numerical techniques such as the Gauss-Newton or Levenberg-Marquardt method. Efficient ways to calculate the Jacobian matrix needed in the implementation of these methods can be found in [12].

B. Cramér-Rao Bound

The Cramér-Rao bound is given by [11] as

$$\mathrm{cov}(\hat{\boldsymbol{\theta}}_n) \succeq \mathcal{I}_{\boldsymbol{\theta}_n}^{-1}, \tag{14}$$

where the Fisher information matrix is

$$\mathcal{I}_{\boldsymbol{\theta}_n} = \sigma^{-2}\mathbf{K}^\top(\mathbf{I}-\mathbf{P})\mathbf{K} \tag{15}$$

and $\mathbf{K} = \frac{d\mathbf{H}(\boldsymbol{\theta}_n)\boldsymbol{\theta}_l}{d\boldsymbol{\theta}_n}$. As the bound depends on the true model parameters, it cannot be evaluated directly from a sequence of real-world measurements. However, the bound can be approximated by using the estimated parameters, and thereby used as an indicator of the accuracy of the displacement estimate. Further, the bound can be used to gain insight into the basic properties of the displacement estimation problem. To do so, the bound for the one dimensional case will be analyzed next.

Consider an array consisting of N single axis magnetometers equidistantly mounted in a straight line; refer to Fig. 2 for an illustration. Assume that the array moves along a straight line and is aligned with the direction of motion. Further, assume that the magnetic field locally can be modelled by the linear model, i.e., $\mathbf{M}(r;\boldsymbol{\theta}) = \theta_2 r + \theta_1$. Then the Cramér-Rao bound in (14) simplifies to

$$\mathrm{var}(\hat{x}) \geq \frac{2\sigma^2}{N\theta_2^2}\left(1 + \frac{3}{N^2-1}\left(\frac{x}{d}\right)^2\right). \tag{16}$$

As can be seen, the bound is proportional to the ratio between the noise variance and the rate of change of the field. Hence, if the field does not change, the accuracy degrades quickly.

From a positioning perspective, it is generally more interesting to talk about the displacement estimation error in terms of percentages of the traveled distance than in terms of the variance of the distance estimate. Normalizing the variance with the squared displacement and simplifying yields

$$\frac{\mathrm{var}(\hat{x})}{x^2} \geq \underbrace{\frac{2\sigma^2}{N\theta_2^2}}_{\sim 1/\mathrm{SNR}}\left(\frac{1}{x^2} + \underbrace{\frac{3}{(N^2-1)d^2}}_{\sim 1/(\text{length of array})^2}\right) \tag{17}$$

That is, for long displacements the error in terms of a percentage of the traveled distance is inversely proportional to the "signal-to-noise" ratio and the length of the array. Hence, to optimize the estimation accuracy the size of array should be as large as possible, but still small enough so that the model of the magnetic field is valid.

IV. Experiment and Results

An example of the variations in the magnetic field inside an office building is shown in Fig. 3. Visual inspection shows that on a length scale of approximately 0.5 m the field variations can be well approximated using a second or third order polynomial model. This indicates that an array in which the sensors are distributed to cover a square with a side of a few decimeters should be used if aiming to obtain magnetic odometry using the proposed method. Unfortunately, we currently only have access to the array depicted in Fig. 1, in which the sensors are distributed over a square with a side of approximately 2 cm.

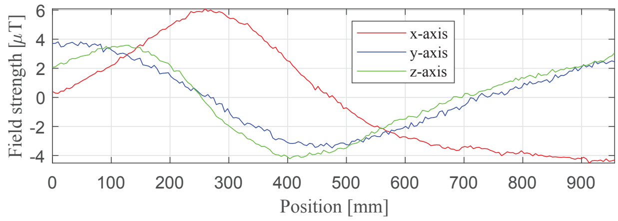

Fig. 3. Example of the variations in the local magnetic field inside an office building. The mean value of each field components has been removed to better visualize the variations in the field.

The following experiment was conducted with an artificially created magnetic field. The array was mounted on a linear actuator that, in steps of 9.58 mm, was used to move the array along a straight line. At each step j a set of magnetometer readings $\{\mathbf{y}_j^{(i)}\}_{i=1}^N$ was collected, where each $\mathbf{y}_j^{(i)}$ was calculated as the average value of 800 time samples of magnetometer data; the resulting noise standard deviation $\sigma \approx 0.1\,\mu$T. To get faster variations in the magnetic field, three small magnets were placed at random along the path of the linear actuator. The resulting magnetic field as a function of the position of the array is depicted in Fig. 4.

The experiment was repeated five times. The data from each experiment was divided into two parts, each part containing the data from the sixteen sensors on the top and the bottom of the array, respectively. That is, from each experiment two data sets containing data from two planar arrays were obtained. The resulting ten data sets where subsequently processed using the proposed estimator together with a second order model for the magnetic field variations; the rotation ϕ was assumed to be known. The mean and standard deviation of the individual displacement estimation errors as a function of the position of the array was then calculated. The results are shown Fig. 5. Also shown is the Cramér-Rao bound (calculated using the estimated parameter values) in terms of the $\pm 3\sqrt{\mathrm{tr}(\mathcal{I}_{\boldsymbol{\theta}_n}^{-1})}$ values. Further, for comparison, the estimation accuracy obtained when directly solving (1) using Euler's method was also evaluated. That is, the displacement was estimated as

$$\hat{\mathbf{x}} = \left(\frac{d\mathbf{m}}{d\mathbf{r}}\right)^{-1}\frac{1}{N}\sum_{i=1}^{N}(\mathbf{y}_1^{(i)} - \mathbf{y}_0^{(i)}), \tag{18}$$

where the Jacobian of the field $d\mathbf{m}/d\mathbf{r}$ was estimated using a second order polynomial model. The result is shown by the dashed black line in Fig. 5.

The results show that when there are large variations in the magnetic field the displacement can be estimated using the proposed method with sub-millimeter accuracy. This corresponds to a few percent of the true displacement of 9.58 mm. When the magnetic field flattens out, i.e., the field starts to lose sufficient excitation, towards the end of the trajectory the performance of the proposed estimator declines quickly and the estimation error is in the order of 50 %

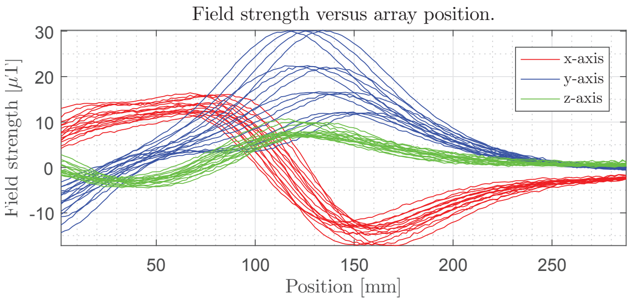

Fig. 4. Field measured by the sensor array during the experiment.

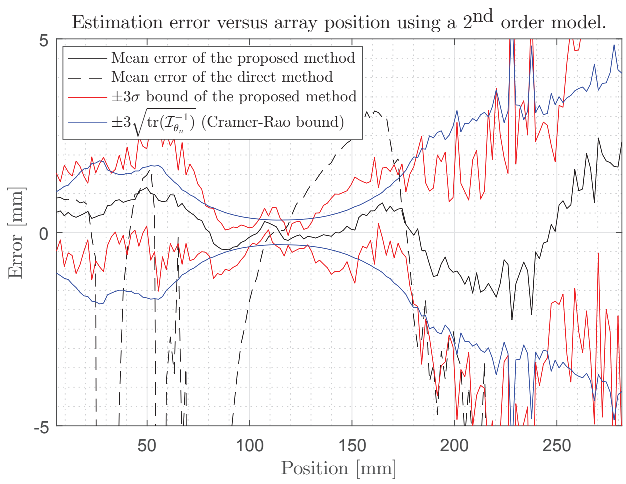

Fig. 5. Mean and standard deviation (in terms of the 3σ bound) of the estimation error for the proposed method. Also shown is the mean estimation error of the direct method, which is based upon solving differential equation (1). The Cramér-Rao bound for the estimation error is also displayed.

of the true displacement. Further, the results show that the estimation accuracy obtained when using the estimator in (18) is substandard. Moreover, it can be seen that the estimation accuracy predicted by the Cramér-Rao bound is in agreement with the empirically calculated estimation.

V. Summary, Discussion, and Conclusions

A model-based approach to magnetic odometry, i.e., estimation of the displacement of a magnetometer array moving through a spatially varying magnetic field, has been presented. Further, based upon a curl and divergence free polynomial model for the magnetic field, a maximum likelihood estimator for the displacement has been derived. Moreover, an identifiability analysis of the signal model when using a second order polynomial shows that it is sufficient to have magnetometer triads mounted in a plane to identify all the model parameters. This greatly simplifies the practical design of the array, as it can be constructed on a single printed circuit board.

The performance of the estimator has been experimentally evaluated using a miniaturized sensor array with the form factor $2 \times 2\,$cm and an artificially created magnetic field with a rate of change of up to $6\,\mu$T/cm. The results show that where there are sufficient variations in the magnetic field the displacement can be estimated with an error of a few percent. Translated into a typical indoor environment where magnetic field variations on the order of a few micro-Tesla per decimeter are common, the results indicate that an odometry accuracy of a few percentage of the traveled distance should be achievable when using an array built out of low-noise magnetometer sensors and which has a length scale of 1–3 decimeters. The results also shows that the proposed method clearly outperforms the accuracy of the current standard method, which is based upon solving (1) directly.

Another benefit of the proposed method is that the formulation fits well into a Bayesian filtering framework. This makes it easy to combine the magnetic odometry measurements with, e.g., inertial measurements, to create a system that would be able to provide accurate localization in a wide variety of indoor environments.

Future work will therefore be focused on evaluating the proposed method using a full size sensor array that is observing only the natural variations in magnetic field. Further, as the proposed method can also be used with other magnetic field models than the one presented, the method will be tested using, e.g., the curl and divergence Gaussian process model in [7]. Moreover, as the identifiability analysis shows that the rotation of the array can also be determined, it will be investigated how well this can be estimated.

References

[1] A. Solin, S. Särkkä, J. Kannala, and E. Rahtu, "Terrain navigation in the magnetic landscape: Particle filtering for indoor positioning," in *2016 European Navigation Conference (ENC)*, May 2016, pp. 1–9.

[2] M. Kok and A. Solin, "Scalable magnetic field SLAM in 3D using gaussian process maps," *CoRR*, vol. abs/1804.01926, 2018. [Online]. Available: http://arxiv.org/abs/1804.01926

[3] D. Vissiere, A. Martin, and N. Petit, "Using distributed magnetometers to increase IMU-based velocity estimation into perturbed area," in *46th IEEE Conf. on Decision and Control*, New Orleans, LA, Dec. 2007.

[4] E. Dorveaux, T. Boudot, M. Hillion, and N. Petit, "Combining inertial measurements and distributed magnetometry for motion estimation," in *Proc. of the 2011 American Control Conf.*, San Francisco, CA, Jun. 2011.

[5] E. Dorveaux and N. Petit, "Presentation of a magneto-inertial positioning system: navigating through magnetic disturbances," in *Int. Conf. on Indoor Positioning and Indoor Navigation (IPIN)*, Guimaraes, Portugal, Sep. 2011.

[6] C. I. Chesneau, M. Hillion, and C. Prieur, "Motion estimation of a rigid body with an EKF using magneto-inertial measurements," in *Int. Conf. on Indoor Positioning and Indoor Navigation (IPIN)*, Alcala de Henares, Spain, Oct. 2016.

[7] N. Wahlström, M. Kok, T. B. Schön, and F. Gustafsson, "Modeling magnetic fields using Gaussian processes," in *IEEE Int. Conf on Acoustics, Speech and Signal Processing ICASSP*, Vancouver, BC, May 2013.

[8] T. Kailath, A. H. Sayed, and B. Hassibi, *Linear Estimation*. Prentice Hall, 2000.

[9] L. Ljung, *System Identification — Theory For the User*, 2nd ed. Prentice-Hall, 1999.

[10] E. Dorveaux, "Magneto-inertial navigation: principles and application to an indoor pedometer," Ph.D. dissertation, Paris Institute of Technology, 2011.

[11] S. M. Kay, *Fundamentals of Statistical Signal Processing: Estimation Theory*. Prentice Hall, 1993.

[12] G. Golub and V. Pereyra, "Separable nonlinear least squares: the variable projection method and its applications," *Inverse Problems*, vol. 19, no. 2, pp. R1–R26, 2003.